Synthesis of Finely Controllable Sizes of Au Nanoparticles on a Silica Template and Their Nanozyme Properties

Bomi Seong
Konkuk University
Jaehi Kim
Konkuk University
Wooyeon Kim
Konkuk University
Sang Hun Lee
Hanbat National University
Xuan-Hung Pham (phamricky@gmail.com)
Konkuk University https://orcid.org/0000-0002-4927-7102
Bong-Hyun Jun
Konkuk University

Research

Keywords: Nanoparticles , precise synthesis , tetramethyl benzidine

Posted Date: June 14th, 2021

DOI: https://doi.org/10.21203/rs.3.rs-589538/v1

Abstract

The precise synthesis of fine-sized nanoparticles is critical for realizing the advantages of nanoparticles for various applications. We developed a technique for preparing finely controllable sizes of gold nanoparticles (Au NPs) on a silica template using the seed-mediated growth and interval dropping methods. These Au NPs, embedded on silica nanospheres (SiO_2@Au NPs), possess peroxidase-like activity as nanozymes and have several advantages over other nanoparticle-based nanozymes. We confirmed their peroxidase activity; in addition, factors affecting the activity were investigated by varying the reaction conditions such as concentrations of tetramethyl benzidine and H_2O_2, pH, particle amount, reaction time, and termination time. We found that SiO_2@Au NPs are highly stable under long-term storage and reusable for five cycles. Our study, therefore, provides a novel method for controlling the properties of nanoparticles and for developing nanoparticle-based nanozymes.

Introduction

Enzymes are biocatalysts that play an important role in living systems. However, they are expensive, difficult to store, laborious to produce, and are easily denatured in external environments from varying temperature, pH, and chemical stressors [1, 2]. These drawbacks critically limit their practical uses [3].

To overcome the above limitations, nanozymes have been developed as a new alternative to enzymes [1, 4]. Nanozymes are nanomaterials that possess an intrinsic enzyme-like activity and have advantages such as stability in external environments, reasonable costs, and good catalytic activity [1, 2, 5–9].

Since the discovery of the unique peroxidase-like activity of Fe_3O_4 magnetic nanoparticles (NPs) by Yan's group in 2007, numerous researchers around the world have gained an interest in nanozymes made of metal nanomaterials [10]. Metal nanomaterials, including gold (Au) NPs, platinum NPs, iron oxide NPs, cerium oxide NPs, manganese oxide NPs, and copper oxide NPs began to be used as nanozymes [5, 6, 10–15]. Most of them have exhibited enzyme-like activities like that of peroxidases, catalases, oxidases, and superoxide oxidases [1–3, 5, 6, 10, 14–22].

Among the various metal nanomaterials, Au NPs have attracted the most attention because of their outstanding catalytic properties and advantages [23–35]. Au NPs can be synthesized easily and are stable [36, 37]. In addition, the physical/chemical properties of Au NPs can be controlled by controlling their size and shape [24, 26, 33, 35]. These NPs are also highly biocompatible and are easy to functionalize [24, 30, 35, 38–42]. However, gold is not cheap, and the catalytic reactions depend on the surface area of the NPs. Fine-sized NPs can be cost-effective, but are difficult to separate for reuse [1, 3, 8–10, 17, 43, 44]. The development of a structure that uses small amounts of gold to acquire a large surface area, while still being easily separated, might prove to be a highly useful material in the field of nanozymes. A nanostructure where Au NPs are assembled onto a silica (SiO_2) sphere core was developed by the Halas group in 1998 [45]. The chemical and optical properties of the Au NP-embedded SiO_2 structure can be changed by simply controlling the diameter of the core and layered nanoparticles [46–

51]. The NP-embedded SiO_2 nanostructures are also cost-effective since only small amounts of expensive Au NPs are embedded onto the silica core, and they are easily separated from the reaction solution with the SiO_2 core.

Au NP-assembled SiO_2 nanostructures have been investigated in various fields [44, 50, 52–62] and have been found to have many merits due to the combined properties of Au NPs and of the silica core, simultaneously utilizing the outstanding and unique features of Au NPs as well as the inert and versatile feature of SiO_2 [53, 55, 56, 63]. In addition, the absorbance spectra of the nanostructures can be tuned across the visible and infrared regions by controlling the size of the Au NPs [38, 39, 64, 65]. Due to these properties, the Au NP-assembled SiO_2 nanostructures have broad applications. While there are many possible approaches for the control of the size and density of Au NPs on a template surface, a method of synthesis for those nanostructures has not yet been established [46, 48–50, 64, 65]. For this reason, the low density and non-uniform morphology of Au NPs on nanostructures remain a considerable challenge [46, 48–50]. There is, therefore, a need for the development of an improved method for preparing Au NP-assembled silica nanostructures.

Our group recently developed SiO_2@Au nanostructures in which Au NPs were densely immobilized on the surface of a SiO_2 nanosphere [66]. For this nanostructure, the SiO_2 nanosphere was used as a template and the Au NPs were uniformly and densely introduced on it using the seed-mediated growth method (Fig. 1). SiO2@Au nanostructures have enhanced separation and re-dispersion properties and are more stable during surface modification than Au NPs. Also, they have shown potential as effective nanozymes. In this study, besides introducing dense and uniform Au NPs onto the SiO_2 nanospheres, we also developed a facile method to very precisely control the size of Au NPs on the SiO_2 surface and investigated their optical and catalytic characteristics by controlling the size of the Au NPs. Furthermore, various factors affecting the peroxidase-like activity of SiO_2@Au NPs were also studied.

Materials And Methods

Chemicals and reagents

Tetraethylorthosilicate (TEOS), tetrakis(hydroxymethyl)phosphonium chloride (THPC), chloroauric acid ($HAuCl_4$), 3-aminopropyltriethoxysilane (APTS), AA, PVP (MW 40,000), and TMB were purchased from Sigma-Aldrich (St. Louis, MO, USA). Ammonium hydroxide (NH_4OH, 27%), ethyl alcohol (EtOH, 99.9%), sodium hydroxide (NaOH), and sulfuric acid (H_2SO_4) were purchased from Samchun (Seoul, Korea). Hydrogen peroxide (H_2O_2) was purchased from Daejung (Siheung, Gyeonggi-do, Korea). Phosphate buffer saline containing 0.1% Tween 20 (PBST, pH 7.4) was purchased from Dynebio (Seongnam, Gyeonggi-do, Korea)

Characterization

The transmission electron microscope (TEM) images of the samples were taken using a JEM-F200 multi-purpose electron microscope (JEOL, Akishima, Tokyo, Japan) with a maximum accelerated voltage of 200 kV. The UV-Vis absorption spectra of the sample were measured by an Optizen POP UV/Vis spectrometer (Mecasys, Seoul, Korea). The centrifugation of samples was performed using a microcentrifuge 1730R (LaboGene, Lyngen, Denmark).

Synthesis of gold nanoparticles (Au NPs) assembled SiO_2 nanostructure (SiO_2@Au NPs)

The SiO_2@Au NPs were synthesized according to the previous report [66]. The colloidal Au was prepared by stirring 47.5 mL of water, 0.5 mL of 0.2 M NaOH, 12 μL of THPC, and 1 mL of 50 mM $HAuCl_4$ for 1 h. Silica nanospheres (~ 160 nm) were prepared by using the modified Stöber method [83]. Briefly, 40 mL of EtOH, 1.6 mL TEOS, and 3 mL of NH_4OH were allowed to react with each other for 20 h. The amino group was introduced to the surface of 2 mg SiO_2 NPs by treating them with 62 μL of APTS. The aminated SiO_2 NPs were incubated with colloidal Au (~ 2.5 nm) for 12 h. After several cycles of centrifugation of the mixture at 8500 rpm for 10 min, 2 mg of Au-seeded SiO_2 NPs were obtained and dispersed in 2 mL of PVP solution (1 mg/mL of PVP in water). Subsequently, 200 μL of Au-seeded SiO_2 NPs suspension was added to 9.8 mL of PVP solution. Twenty microliters of 10 mM $HAuCl_4$ solution (in water, Au^{3+} precursor) and 40 μL of AA solution, (10 mM AA in water, reducing agent) were added to the mixture in sequence. The reaction mixture was stirred for 5 min. To control the size of the Au NPs on the surface of the Au-seeded SiO_2 nanospheres, 10 mM of Au^{3+} precursor and AA were added. Until the concentrations of Au^{3+} reached 50, 100, 150, 200 and 300 μM in the various mixtures, the same volumes of Au^{3+} precursor and AA were repeatedly added every 5 min. The SiO_2@Au NPs were washed several times with centrifugation at 8500 rpm for 10 min. The washed SiO_2@Au NPs were dispersed in 1 mL of 0.1% PBST solution to obtain a 0.2 mg/mL SiO_2@Au NP suspension.

Peroxidase-like activity of SiO_2@Au

To verify the peroxidase-like activity of SiO_2@Au NPs, 100 μL of TMB solution (1 mM in EtOH) and 100 μL of the various concentrations of SiO_2@Au NPs (50, 100, 150, 200, and 300 μM, respectively) were added to 700 μL of pH 4 buffer. Then, freshly prepared 100 μL of H_2O_2 solution (2 M in pH 4 buffer) was added and the mixture was incubated for 30 min at room temperature. To terminate the reaction, 500 μL of 1 M H_2SO_4 was added to each mixture and incubated for 10 min. The absorbance of the mixture at 350–800 nm was measured by using the UV-Vis spectrometer.

Peroxidase-like activity of SiO_2@Au in various reaction conditions

TMB concentration

All assays of peroxidase-like activity were carried out in 1.5 mL Eppendorf tubes at room temperature. The TMB solutions were prepared in EtOH at various concentrations (1, 2, 4, 6, 8, and 10 mM, respectively). Then, 100 μL of each TMB solution, 100 μL of 2 M H_2O_2, and 100 μL of SiO_2@Au (0.2 mg/mL) were added to 700 μL of pH 4 buffer. The final concentrations of TMB in the reaction mixture were 0.1, 0.2, 0.4, 0.6, 0.8, and 1.0 mM. After incubating the mixture for 30 min, 500 μL of 1 M H_2SO_4 was added to terminate the reaction. The absorbance of mixtures was measured using a UV-Vis spectrometer.

H_2O_2 concentration

Various concentrations of H_2O_2 solutions (1, 2, 3, and 4 M) were prepared. Next, 100 μL of 6 mM TMB solution, 100 μL of each H_2O_2 solutions, and 100 μL of SiO_2@Au (0.2 mg/mL) were added to 700 μL of pH 4 buffer. The final concentrations of H_2O_2 in the mixtures were 100, 200, 300, and 400 mM respectively. After incubating the mixtures for 30 min at room temperature, 500 μL of 1 M H_2SO_4 was added to each to terminate the reaction.

pH value of the buffer

Buffers of pH 3, 4, 5, 6, 7, and 8 were prepared. Next, 700 μL of prepared each buffer were added, followed by adding 100 μL of TMB solution, 100 μL of 2 M H_2O_2 solution, and 100 μL of SiO_2@Au NPs (0.2 mg/mL). The mixtures were incubated for 30 min and the reaction was terminated using 500 μL of 1 M H_2SO_4.

Amount of SiO_2@Au NPs

All reagents including 100 μL of 6 mM TMB solution, 100 μL 2 M H_2O_2 solution, and 700 μL pH 4 buffer were added into tubes. Then 1, 5, 10 15, 20, 25, 30, 40, and 50 μg of SiO_2@Au was dispersed in 100 μL PBST each and added to the mixtures, followed by incubation and termination.

Reaction time

To investigate the effect of reaction time on their peroxidase-like activity, the mixtures containing 100 μL of 6 mM TMB solution, 100 μL of SiO_2@Au (0.2 mg/mL), and 100 μL of 2 M H_2O_2 solution were added to 700 μL of pH 4 buffer. Next, the mixtures were incubated for 0, 5, 10, 15, 20, 25, and 30 min respectively and terminated using 1 M H_2SO_4.

Termination time

Mixtures including 700 μL of pH 4 buffer, 100 μL of 6 mM TMB solution, 100 μL of SiO_2@Au (0.2 mg/mL), and 100 μL of 2 M H_2O_2 solution were prepared and incubated for 30 min. After adding 500 μL of 1 M H_2SO_4, each sample was incubated for 0, 5, 10, 15, 20, 25, and 30 min to terminate the reaction.

Long-term stability of peroxidase-like activity

To investigate the long-term stability of peroxidase-like activity of SiO_2@Au, the experiment was repeated every day for 2 weeks and on the 31st day after their fabrication. The experimental procedures were conducted as follows: adding 100 μL of 6 M TMB solution, 100 μL of SiO_2@Au (0.2 mg/mL), and 100 μL of 2 M H_2O_2 solution to 700 μL of pH 4 buffer; 30 min reaction time; 10 min for termination using 500 μL of 1 M H_2SO_4.

Reusability as nanozymes

To investigate the reusability of SiO_2@Au, the peroxidase assay was performed according to the mentioned procedures. After the assay was done, the SiO_2@Au NPs were collected using centrifugation at 10,000 rpm for 10 min and the absorbance of the supernatant at 453 nm was measured by using a UV-vis spectrometer. The peroxidase assay was repeated with the collected SiO_2@Au NPs.

Results And Discussion

Preparation of size-controlled Au NPs-assembled silica nanostructures (SiO_2@Au NPs)

The SiO_2@Au NPs were prepared by using seed-mediated growth synthesis, consisting of two steps: embedding Au seeds on the SiO_2 surface, and growth of the Au NPs via the addition of an Au^{3+} precursor and reductant in intervals [45, 53]. First, the Au seeds (~ 2.5 nm) were prepared using an Au^{3+} precursor ($HAuCl_4$) and tetrakis(hydroxymethyl)phosphonium chloride (THPC). Then, the Au seeds were incubated with aminated SiO2 nanospheres (~ 160 nm) to obtain Au-seeded SiO2 nanospheres as previously reported [62, 63, 66–68]. On the Au-seeded SiO2 nanospheres, the reduction of the Au3 + precursor was directly conducted using ascorbic acid (AA) which is a mild reducing agent, in the presence of polyvinylpyrrolidone (PVP) as a stabilizer. In these mildly reducing conditions, the progress of the growth stage is much slower than in strongly reducing conditions, making it easier to control the growth procedure [36]. A low concentration of the Au^{3+} precursor and AA were added onto the Au-seeded SiO_2 in 5 min intervals until the desired concentrations for fine control over the size of the Au NPs are attained. The amounts are indicated in Table 1.

First, numerous small Au NPs (~ 2.5 nm) were attached throughout the SiO_2 surface as seeds for the further growth of Au NPs, as shown in Fig. 1. Subsequently, various concentrations of the Au^{3+} precursor were added to the Au-seeded SiO_2 nanospheres at intervals; the size of the Au NPs grew larger as the

Au^{3+} concentration was increased. Also, the size of the Au NPs on the SiO_2 nanospheres was precisely controlled with high levels of density and uniformity, which were confirmed clearly as shown in Fig. 1. When the size of the Au NPs increased, the color of the solution changed in the order pale brown, then pink, purple, dark blue, and finally black (Fig. 2a). These changes occurred depending on the size and shape of the NPs due to their localized surface plasmon resonance (LSPR) [37, 46, 48]. When nanoparticles are close to one another, the absorption spectra of proximally located nanoparticles red-shifts considerably from that of solitary particles [65, 69]. Increasing the space between the particles reduces the shift [69]. Mie's theory accounts for how increasing nanoparticle diameters induces the absorption spectra to red-shift by changing the electric surface charge density of the NPs [70]. The results of our study showed that the growth of Au NPs on SiO2@Au was controlled well by the color change of the particle suspension, transmission electron microscopy (TEM) images, and absorbance according to the above-mentioned theories. The absorption spectra of SiO_2 showed that the absorbance band was red-shifted and broadened upon an increase in the concentration of the Au^{3+} precursor, indicating the formation of larger Au NPs, which change the proximate interparticle distance (Fig. 2b–c). In the absorbance band of SiO_2@Au NPs-treated 0 μM Au^{3+} precursor, no peak was observed due to the exceedingly tiny size of the Au NPs. On the other hand, 50, 100, 150, 200, and 300 Au^{3+} precursor-treated SiO_2@Au showed peaks at 543, 571, 593, 619, and 632 nm respectively (Fig. 2c). Also, the absorbance bandwidth broadened as the size of the Au NPs was increased.

Figure 2: (a) Optical images and (b) Size of Au NPs, and (c) UV-Vis absorption spectra of SiO_2@Au NPs fabricated in various concentrations of Au^{3+} precursor: (i) 0 μM, (ii) 50 μM, (iii) 100 μM, (iv) 150 μM, (v) 200 μM, and (vi) 300 μM.

Table 1
Amount of material controlling TEM) images of gold-embedded silica nanospheres (SiO_2@Au NPs) and its effect.

Sample	Au-seeded SiO_2 spheres (mg)	Au precursor (μM)	Ascorbic acid (μM)	Au size (nm)	λ_{max} (nm)	Absorbance intensity at λ_{max} (a.u.)	Suspension color
i	200	0	0	1.41	-	-	Pale brown
ii	200	50	100	4.33	543	0.27	Pink
iii	200	100	200	6.42	571	0.54	Purple
iv	200	150	300	7.33	593	0.87	Dark blue
v	200	200	400	9.56	619	1.20	Dark blue
vi	200	300	600	15.27	632	1.27	Dark blue
Sample numbers correspond to those mentioned in Fig. 1.							

Verification of the peroxidase-like activity of SiO_2@Au NPs

The peroxidase-like activity of SiO_2@Au NPs was evaluated through oxidation of a 3,3′,5,5′-tetramethylbenzidine (TMB) substrate. The TMB oxidation reaction involves the transfer of two electrons that each produce a clear color change. When the first electron is transferred to form TMB^+ via oxidization of TMB, the TMB solution changes from colorless to blue. Since TMB^+ is quite unstable in an acidic environment, it further oxidizes to TMB^{2+} when the second electron is transferred; TMB^{2+} is stable in acidic conditions, exhibiting a yellow color and a maximum absorption peak at 453 nm (Fig. 3a)[71].

To confirm the peroxidase-like activity of the SiO_2@Au NPs, TMB + H_2O_2, TMB + SiO_2@Au NPs, and TMB + H_2O_2 + SiO_2@Au NPs were prepared in a pH 4 buffer for the peroxidase assay. The TMB + H_2O_2 solution was colorless and an absorbance peak at 453 nm did not appear, as shown in Fig. 2b,c. This result indicated that peroxidase-like activity did not occur in the absence of SiO_2@Au. Next, the color of the TMB + SiO_2@Au NP sample was entirely on account of the SiO_2@Au NPs, displaying an absorbance band with a maximum peak at 630 nm. However, a yellow solution and an absorbance band at 453 nm were observed in the TMB + H_2O_2 + SiO_2@Au NPs sample. These results showed that SiO_2@Au NPs catalyzed TMB oxidation in the presence of H_2O_2, indicating that a peroxidase-like reaction occurred due to the peroxidase-mimicking property of SiO_2@Au NPs.

The peroxidase-like activity depends on the size of the Au NPs of the SiO_2@Au NPs

To investigate the correlation between the size of the Au NPs and the peroxidase-like activity of SiO_2@Au NPs, various kinds of SiO_2@Au NPs with different Au NPs sizes were prepared. The concentrations of the treated Au^{3+} precursors were 0, 50, 100, 150, 200, and 300 μM each, resulting in the formation of 1.4, 4.3, 6.4, 7.3, 9.5, and 15 nm diameter Au NPs on the SiO_2@Au structures respectively (Table 1, Fig. 2b). Each of these SiO_2@Au NPs was subjected to the TMB assay to estimate their peroxidase-like activity. An absorbance peak at 453 nm was observed in the UV-Vis absorption spectra of all samples, indicating that all of the SiO_2@Au NPs had peroxidase-like activity, irrespective of the size of the Au NPs. However, the SiO_2@Au NPs produced without any $Au3^+$ precursor treatment showed relatively very weak peroxidase-like activity. This may be because the size of the Au NPs on the silica core was too small; there were a large number of vacant spaces on the SiO_2@Au NPs with the given number of Au NPs, providing an insufficient surface area for the reaction between the Au NPs and reactants. On the other hand, SiO_2@Au NPs treated with more than 50 μM Au^{3+} precursor showed high peroxidase-like activity. The size of the Au NPs was rapidly increased when concentrations of Au^{3+} precursor exceeded 50 μM as shown in the TEM images (Fig. 1a). As the size of the Au NPs on the SiO_2@Au NPs was increased, the surface area which can react with reactants also increased. Therefore, the peroxidase-like activity of the SiO_2@Au NPs was increased as the concentrations of the Au^{3+} precursor were increased (Fig. 4a, b). Even though the size of the Au NPs grew as the concentration of the Au^{3+} precursor increased, severe aggregation occurred immediately after the peroxidase reaction in the SiO_2@Au was treated with over 200 μM of the Au^{3+} precursor. Since good dispersibility is an important factor for generating a constant and stable catalytic activity, 150 μM of Au^{3+} precursor-treated SiO_2@Au NPs, which have high peroxidase-like activity without aggregation, was used in the subsequent experiments [72, 73].

Effects of reaction conditions on the peroxidase-like activity of SiO_2@Au NPs

It is known that the catalytic activity of nanozymes is affected by reaction conditions like those associated with an enzyme [10, 32, 74–77]. For this reason, the effect of reaction conditions on the peroxidase-like activity on SiO_2@Au NPs was investigated. The concentration of TMB and H_2O_2, pH of the buffer, the number of SiO_2@Au NPs, reaction time, and termination time were considered in this study. For confirming the effects of TMB concentrations, the concentrations of TMB varied from 0 to 1.0 mM while the other conditions were fixed in the peroxidase assay. The catalytic activity of SiO_2@Au NPs increased until the concentrations of TMB were 0.8 mM; they then decreased at 1.0 mM, because the poor solubility of TMB in an aqueous buffer caused precipitation during the oxidation reaction (Fig. 5a)[78]. In the case of the concentration of hydrogen peroxide, the catalytic activity of SiO_2@Au NPs was increased steeply until reaching 200 mM H_2O_2 and decreased at a concentration of 300 mM H_2O_2. Even though the activity again increased at 400 mM H_2O_2, the rate of increase was lower than 200 mM H_2O_2 (Fig. 5b). Subsequently, various buffers with different pH were subjected to the peroxidase assay. The highest activity was shown under pH 4.0, at which H_2O_2 was more stable and TMB dissolved maximally (Fig. 5c)

[10, 44, 78–81]. The velocity of the catalytic reaction showed the highest value when 20 and 25 μg of SiO_2@Au NPs were treated in the sample where the rest of the conditions were fixed (Fig. 5d). About 25 min was required for the TMB^+ oxidation and 5 min for the termination of the TMB^+ oxidation to obtain stable results (Fig. 5e, f).

Long-term stability and reusability test of SiO_2@Au as nanozyme

SiO_2@Au NPs are substantially more advantageous over enzymes owing to their long-term stability and reusability. Denaturation during storage and their on-off usage are the major defects when using enzymes in practice [1, 2]. To verify the long-term stability of their peroxidase-like activity, the SiO_2@Au NPs were examined by repeating the peroxidase assay every day at the same time for 14 days and on the 31st day after they were produced, keeping them under storage at 25°C in the meantime (Fig. 6a). The results showed that the peroxidase-like activity remained highly stable for at least 30 days after the fabrication of the SiO_2@Au NPs. In sequence, the reusability of the SiO_2@Au NPs as a nanozyme was evaluated through repeated peroxidase assays. Notably, the peroxidase-like activity of SiO_2@Au until the fourth round was 98% of the first cycle level and mildly reduced at the fifth cycle to 89% of the first round. The reusability of SiO_2@Au NPs was significantly high compared to a previous report on an Au NP-embedded silica nanostructure [82]. These results indicate that SiO_2@Au NPs excel not only in being highly reusable but also in separating easily from the reaction mixture.

Conclusions

In summary, we successfully synthesized finely controllably sized Au NPs on the SiO_2 nanosphere (SiO_2@Au) using the seed-mediated growth method and interval dropping method under mild conditions. The effect of the size of Au NPs on the SiO_2@Au NPs was confirmed by the TEM images, color changing of its suspension, and UV-Vis absorption spectra. Moreover, we investigated the factors affecting the peroxidase-like activity of SiO_2@Au NPs such as TMB concentration, H_2O_2 concentration, pH, SiO_2@Au NPs amount, reaction time, and termination time. Furthermore, SiO_2@Au NPs showed high stability during 30 days-long storage time at room temperature and outstanding reusability for five cycles. This work is therefore meaningful for utilizing controllable nanoparticles in various fields and provides a better approach to develop nanoparticle-based nanozymes.

Declarations

Data Availability

All data generated or analyzed during this study are included in this article.

Conflicts of Interest

The authors declare that there is no conflict of interest regarding the publication of this paper.

Funding Statement

This work was supported by the KU Research Professor Program of Konkuk University and funded by the Ministry of Science and ITC [NRF-2019R1G1A1006488] and by the Ministry of Education [NRF-2018R1D1A1B07045708].

Acknowledgments

The authors are grateful for the financial support from the NRF of Korea. Further, the author gives thanks for the financial support from Konkuk University.

Ethics declarations

Ethics approval and consent to participate.

Not applicable for this study.

Consent for publication

We give our consent for the manuscript to be published in Journal of Nanobiotechnology.

Author Contributions

Conceptualization, Xuan-Hung Pham, and Bong-Hyun Jun; methodology, Bomi Seong, and Xuan-Hung Pham; investigation, Bomi Seong, and Wooyeon Kim; formal analysis, Jaehi Kim; software, Sang Hun Lee; writing—original draft preparation, Bomi Seong, Jaehi Kim; writing—review and editing, Xuan-Hung Pham, and Bong-Hyun Jun; supervisor, Bong-Hyun Jun. All authors have read and agreed to the published version of the manuscript.

References

1. Wei H, Wang E. Nanomaterials with enzyme-like characteristics (nanozymes): next-generation artificial enzymes. Chem Soc Rev. 2013;42:6060–93. doi:10.1039/C3CS35486E.

2. Manea F, Houillon FB, Pasquato L, Scrimin P, Nanozymes. Gold-Nanoparticle-Based Transphosphorylation Catalysts. Angew Chem Int Ed. 2004;43:6165–9. doi:https://doi.org/10.1002/anie.200460649.
3. Wei H, Wang E. Fe3O4 Magnetic Nanoparticles as Peroxidase Mimetics and Their Applications in H2O2 and Glucose Detection. Anal Chem. 2008;80:2250–4. doi:10.1021/ac702203f.
4. Antuña-Jiménez D, Blanco-López MC, Miranda-Ordieres AJ, Lobo-Castañón MJ. Artificial enzyme with magnetic properties and peroxidase activity on indoleamine metabolite tumor marker. Polymer. 2014;55:1113–9. doi:https://doi.org/10.1016/j.polymer.2014.01.037.
5. Zhang K, Hu X, Liu J, Yin J-J, Hou S, Wen T, He W, Ji Y, Guo Y, Wang Q, et al. Formation of PdPt Alloy Nanodots on Gold Nanorods: Tuning Oxidase-like Activities via Composition. Langmuir. 2011;27:2796–803. doi:10.1021/la104566e.
6. He W, Jia H, Li X, Lei Y, Li J, Zhao H, Mi L, Zhang L, Zheng Z. Understanding the formation of CuS concave superstructures with peroxidase-like activity. Nanoscale. 2012;4:3501–6. doi:10.1039/C2NR30310H.
7. Ju H. Sensitive biosensing strategy based on functional nanomaterials. Science China Chemistry. 2011;54:1202. doi:10.1007/s11426-011-4339-2.
8. Celardo I, Pedersen JZ, Traversa E, Ghibelli L. Pharmacological potential of cerium oxide nanoparticles. Nanoscale. 2011;3:1411–20. doi:10.1039/C0NR00875C.
9. Kotov NA. Inorganic Nanoparticles as Protein Mimics. Science. 2010;330:188. doi:10.1126/science.1190094.
10. Gao L, Zhuang J, Nie L, Zhang J, Zhang Y, Gu N, Wang T, Feng J, Yang D, Perrett S, et al. Intrinsic peroxidase-like activity of ferromagnetic nanoparticles. Nat Nanotechnol. 2007;2:577–83. doi:10.1038/nnano.2007.260.
11. Cortie MB, Van Der Lingen E. Catalytic gold nano-particles. Mater Forum. 2002;26:1–14.
12. Bond GC, Gold. A relatively new catalyst. Gold Bulletin. 2001;34:117–9. doi:10.1007/BF03214823.
13. Asati A, Santra S, Kaittanis C, Nath S, Perez JM. Oxidase-Like Activity of Polymer-Coated Cerium Oxide Nanoparticles. Angew Chem Int Ed. 2009;48:2308–12. doi:https://doi.org/10.1002/anie.200805279.
14. Chen W, Chen J, Feng Y-B, Hong L, Chen Q-Y, Wu L-F, Lin X-H, Xia X-H. Peroxidase-like activity of water-soluble cupric oxide nanoparticles and its analytical application for detection of hydrogen peroxide and glucose. Analyst. 2012;137:1706–12. doi:10.1039/C2AN35072F.
15. Wang J, Zhao H, Song J, Zhu T, Xu W. Structure-Activity Relationship of Manganese Oxide Catalysts for the Catalytic Oxidation of (chloro)-VOCs. Catalysts. 2019;9:726.
16. Karakoti A, Singh S, Dowding JM, Seal S, Self WT. Redox-active radical scavenging nanomaterials. Chem Soc Rev. 2010;39:4422–32. doi:10.1039/B919677N.
17. Jiao X, Song H, Zhao H, Bai W, Zhang L, Lv Y. Well-redispersed ceria nanoparticles: Promising peroxidase mimetics for H2O2 and glucose detection. Anal Methods. 2012;4:3261–7.

doi:10.1039/C2AY25511A.

18. Zhang X-Q, Gong S-W, Zhang Y, Yang T, Wang C-Y, Gu N. Prussian blue modified iron oxide magnetic nanoparticles and their high peroxidase-like activity. J Mater Chem. 2010;20:5110–6. doi:10.1039/C0JM00174K.
19. Chaudhari KN, Chaudhari NK, Yu J-S. Peroxidase mimic activity of hematite iron oxides (α-Fe2O3) with different nanostructures. Catal Sci Technol. 2012;2:119–24. doi:10.1039/C1CY00124H.
20. Dutta AK, Maji SK, Srivastava DN, Mondal A, Biswas P, Paul P, Adhikary B. Peroxidase-like activity and amperometric sensing of hydrogen peroxide by Fe2O3 and Prussian Blue-modified Fe2O3 nanoparticles. J Mol Catal A: Chem. 2012;360:71–7. doi:https://doi.org/10.1016/j.molcata.2012.04.011.
21. Comotti M, Della†Pina C, Falletta E, Rossi M. Aerobic Oxidation of Glucose with Gold Catalyst: Hydrogen Peroxide as Intermediate and Reagent. Adv Synth Catal. 2006;348:313–6. doi:https://doi.org/10.1002/adsc.200505389.
22. Shen X, Liu W, Gao X, Lu Z, Wu X, Gao X. Mechanisms of Oxidase and Superoxide Dismutation-like Activities of Gold, Silver, Platinum, and Palladium, and Their Alloys: A General Way to the Activation of Molecular Oxygen. J Am Chem Soc. 2015;137:15882–91. doi:10.1021/jacs.5b10346.
23. Medley CD, Smith JE, Tang Z, Wu Y, Bamrungsap S, Tan W. Gold Nanoparticle-Based Colorimetric Assay for the Direct Detection of Cancerous Cells. Anal Chem. 2008;80:1067–72. doi:10.1021/ac702037y.
24. Popovtzer R, Agrawal A, Kotov NA, Popovtzer A, Balter J, Carey TE, Kopelman R. Targeted Gold Nanoparticles Enable Molecular CT Imaging of Cancer. Nano Lett. 2008;8:4593–6. doi:10.1021/nl8029114.
25. Fang S-B, Tseng WY, Lee H-C, Tsai C-K, Huang J-T, Hou S-Y. Identification of Salmonella using colony-print and detection with antibody-coated gold nanoparticles. J Microbiol Methods. 2009;77:225–8. doi:https://doi.org/10.1016/j.mimet.2009.02.008.
26. Kim CS, Wilder-Smith P, Ahn Y-C, Liaw L-H, Chen Z, Kwon YJ. Enhanced detection of early-stage oral cancer in vivo by optical coherence tomography using multimodal delivery of gold nanoparticles. J Biomed Opt. 2009;14:034008.
27. Thaxton CS, Elghanian R, Thomas AD, Stoeva SI, Lee J-S, Smith ND, Schaeffer AJ, Klocker H, Horninger W, Bartsch G, et al. Nanoparticle-based bio-barcode assay redefines “undetectable” PSA and biochemical recurrence after radical prostatectomy. *Proceedings of the National Academy of Sciences* 2009, *106*, 18437, doi:10.1073/pnas.0904719106.
28. Zhang J, Wang L, Zhang H, Boey F, Song S, Fan C. Aptamer-Based Multicolor Fluorescent Gold Nanoprobes for Multiplex Detection in Homogeneous Solution. Small. 2010;6:201–4. doi:https://doi.org/10.1002/smll.200901012.
29. Huo Q, Colon J, Cordero A, Bogdanovic J, Baker CH, Goodison S, Pensky MY. A Facile Nanoparticle Immunoassay for Cancer Biomarker Discovery. Journal of Nanobiotechnology. 2011;9:20. doi:10.1186/1477-3155-9-20.

30. Leduc C, Jung J-M, Carney RR, Stellacci F, Lounis B. Direct Investigation of Intracellular Presence of Gold Nanoparticles via Photothermal Heterodyne Imaging. ACS Nano. 2011;5:2587–92. doi:10.1021/nn1023285.
31. Von Maltzahn G, Park J-H, Lin KY, Singh N, Schwöppe C, Mesters R, Berdel WE, Ruoslahti E, Sailor MJ, Bhatia SN. Nanoparticles that communicate in vivo to amplify tumour targeting. Nat Mater. 2011;10:545–52.
32. Wang H, Zheng L, Peng C, Guo R, Shen M, Shi X, Zhang G. Computed tomography imaging of cancer cells using acetylated dendrimer-entrapped gold nanoparticles. *Biomaterials* **2011**, *32*, 2979–2988, doi:https://doi.org/10.1016/j.biomaterials.2011.01.001.
33. Zhang Y, Qian J, Wang D, Wang Y, He S. Multifunctional Gold Nanorods with Ultrahigh Stability and Tunability for In†Vivo Fluorescence Imaging, SERS Detection, and Photodynamic Therapy. Angew Chem Int Ed. 2013;52:1148–51. doi:https://doi.org/10.1002/anie.201207909.
34. Youssef AM, Abdel-Aziz MS, El-Sayed SM. Chitosan nanocomposite films based on Ag-NP and Au-NP biosynthesis by Bacillus Subtilis as packaging materials. Int J Biol Macromol. 2014;69:185–91. doi:https://doi.org/10.1016/j.ijbiomac.2014.05.047.
35. Zhang Z, Wang J, Nie X, Wen T, Ji Y, Wu X, Zhao Y, Chen C. Near infrared laser-induced targeted cancer therapy using thermoresponsive polymer encapsulated gold nanorods. J Am Chem Soc. 2014;136:7317–26.
36. Grzelczak M, Pérez-Juste J, Mulvaney P, Liz-Marzán LM. Shape control in gold nanoparticle synthesis. Chem Soc Rev. 2008;37:1783–91. doi:10.1039/B711490G.
37. Daniel M-C, Astruc D. Gold nanoparticles: assembly, supramolecular chemistry, quantum-size-related properties, and applications toward biology, catalysis, and nanotechnology. Chemical reviews. 2004;104:293–346.
38. Henglein A. Physicochemical properties of small metal particles in solution: "microelectrode" reactions, chemisorption, composite metal particles, and the atom-to-metal transition. The Journal of Physical Chemistry. 1993;97:5457–71. doi:10.1021/j100123a004.
39. Belloni J. Metal nanocolloids. Curr Opin Colloid Interface Sci. 1996;1:184–96. doi:https://doi.org/10.1016/S1359-0294(96)80003-3.
40. Toshima N, Yonezawa T. Bimetallic nanoparticles—novel materials for chemical and physical applications. New J Chem. 1998;22:1179–201. doi:10.1039/A805753B.
41. Brust M, Kiely CJ. Some recent advances in nanostructure preparation from gold and silver particles: a short topical review. Colloids Surf A. 2002;202:175–86. doi:https://doi.org/10.1016/S0927-7757(01)01087-1.
42. Lin Y-C, Yu B-Y, Lin W-C, Lee S-H, Kuo C-H, Shyue J-J. Tailoring the surface potential of gold nanoparticles with self-assembled monolayers with mixed functional groups. J Colloid Interface Sci. 2009;340:126–30. doi:https://doi.org/10.1016/j.jcis.2009.08.014.
43. Fan K, Cao C, Pan Y, Lu D, Yang D, Feng J, Song L, Liang M, Yan X. Magnetoferritin nanoparticles for targeting and visualizing tumour tissues. Nat Nanotechnol. 2012;7:459–64.

doi:10.1038/nnano.2012.90.

44. He W, Zhou Y-T, Wamer WG, Hu X, Wu X, Zheng Z, Boudreau MD, Yin J-J. Intrinsic catalytic activity of Au nanoparticles with respect to hydrogen peroxide decomposition and superoxide scavenging. Biomaterials. 2013;34:765–73. doi:https://doi.org/10.1016/j.biomaterials.2012.10.010.
45. Westcott SL, Oldenburg SJ, Lee TR, Halas NJ. Formation and adsorption of clusters of gold nanoparticles onto functionalized silica nanoparticle surfaces. Langmuir. 1998;14:5396–401.
46. Prodan E, Nordlander P, Halas NJ. Electronic Structure and Optical Properties of Gold Nanoshells. Nano Lett. 2003;3:1411–5. doi:10.1021/nl034594q.
47. Wilhelm P, Stephan D. On-line tracking of the coating of nanoscaled silica with titania nanoparticles via zeta-potential measurements. J Colloid Interface Sci. 2006;293:88–92. doi:10.1016/j.jcis.2005.06.047.
48. Loo C, Lin A, Hirsch L, Lee MH, Barton J, Halas N, West J, Drezek R. Nanoshell-enabled photonics-based imaging and therapy of cancer. Technology in cancer research treatment. 2004;3:33–40. doi:10.1177/153303460400300104.
49. Zhang Y-F, Wang J-H, Ma L, Nan F, Cheng Z-Q, Zhou L, Wang Q-Q. Growth of silver-coated gold nanoshells with enhanced linear and nonlinear optical responses. J Nanopart Res. 2015;17:157. doi:10.1007/s11051-015-2928-2.
50. Lu L, Zhang H, Sun G, Xi S, Wang H, Li X, Wang X, Zhao B. Aggregation-Based Fabrication and Assembly of Roughened Composite Metallic Nanoshells: Application in Surface-Enhanced Raman Scattering. Langmuir. 2003;19:9490–3. doi:10.1021/la034738g.
51. Gawande MB, Goswami A, Asefa T, Guo H, Biradar AV, Peng D-L, Zboril R, Varma RS. Core–shell nanoparticles: synthesis and applications in catalysis and electrocatalysis. Chem Soc Rev. 2015;44:7540–90. doi:10.1039/C5CS00343A.
52. Hiramatsu H, Osterloh FE pH-Controlled Assembly and Disassembly of Electrostatically Linked CdSe – SiO2 and Au – SiO2 Nanoparticle Clusters. *Langmuir* 2003, *19*, 7003–7011, doi:10.1021/la034217t.
53. Xue J, Wang C, Ma Z. A facile method to prepare a series of SiO2@Au core/shell structured nanoparticles. Mater Chem Phys. 2007;105:419–25. doi:https://doi.org/10.1016/j.matchemphys.2007.05.010.
54. Brito-Silva AM, Sobral-Filho RG, Barbosa-Silva R, de Araújo CB, Galembeck A, Brolo AG. Improved synthesis of gold and silver nanoshells. Langmuir. 2013;29:4366–72.
55. Tharion J, Satija J, Mukherji S. Glucose mediated synthesis of gold nanoshells: A facile and eco-friendly approach conferring high colloidal stability. RSC Advances. 2014;4:3984–91. doi:10.1039/C3RA45815F.
56. García-Soto MJ, González-Ortega O. Synthesis of silica-core gold nanoshells and some modifications/variations. Gold Bulletin. 2016;49:111–31. doi:10.1007/s13404-016-0188-2.
57. *Science Advances* **2016**, *2*, e1501554, doi:10.1126/sciadv.1501554.

58. Huang L, Wan J, Wei X, Liu Y, Huang J, Sun X, Zhang R, Gurav DD, Vedarethinam V, Li Y, et al. Plasmonic silver nanoshells for drug and metabolite detection. Nat Commun. 2017;8:220. doi:10.1038/s41467-017-00220-4.
59. Qu H, Tong S, Song K, Ma H, Bao G, Pincus S, Zhou W, O'Connor C. Controllable in Situ Synthesis of Magnetite Coated Silica-Core Water-Dispersible Hybrid Nanomaterials. Langmuir. 2013;29:10573–8. doi:10.1021/la4022867.
60. Kang H, Yang J-K, Noh MS, Jo A, Jeong S, Lee M, Lee S, Chang H, Lee H, Jeon S-J, et al. One-step synthesis of silver nanoshells with bumps for highly sensitive near-IR SERS nanoprobes. Journal of Materials Chemistry B. 2014;2:4415–21. doi:10.1039/C4TB00442F.
61. Hahm E, Kang EJ, Pham X-H, Jeong D, Jeong DH, Jung S, Jun B-H. Mono-6-Deoxy-6-Aminopropylamino-β-Cyclodextrin on Ag-Embedded SiO2 Nanoparticle as a Selectively Capturing Ligand to Flavonoids. Nanomaterials. 2019;9:1349.
62. Shim S, Pham X-H, Cha MG, Lee Y-S, Jeong DH, Jun B-H. Size effect of gold on Ag-coated Au nanoparticle-embedded silica nanospheres. RSC Adv. 2016;6:48644–50.
63. Pham X-H, Hahm E, Kang E, Ha YN, Lee SH, Rho W-Y, Lee Y-S, Jeong DH, Jun B-H. Gold-silver bimetallic nanoparticles with a Raman labeling chemical assembled on silica nanoparticles as an internal-standard-containing nanoprobe. J Alloy Compd. 2019;779:360–6. doi:https://doi.org/10.1016/j.jallcom.2018.11.270.
64. Su K-H, Wei Q-H, Zhang X, Mock J, Smith DR, Schultz S. Interparticle coupling effects on plasmon resonances of nanogold particles. Nano Lett. 2003;3:1087–90.
65. Jain PK, El-Sayed MA. Plasmonic coupling in noble metal nanostructures. Chem Phys Lett. 2010;487:153–64. doi:https://doi.org/10.1016/j.cplett.2010.01.062.
66. Seong B, Bock S, Hahm E, Huynh K-H, Kim J, Lee SH, Pham X-H, Jun B-H. Synthesis of Densely Immobilized Gold-Assembled Silica Nanostructures. Int J Mol Sci. 2021;22:2543.
67. Pham X-H, Hahm E, Kang E, Son BS, Ha Y, Kim H-M, Jeong DH, Jun B-H. Control of Silver Coating on Raman Label Incorporated Gold Nanoparticles Assembled Silica Nanoparticles. Int J Mol Sci. 2019;20:1258.
68. Pham X-H, Hahm E, Huynh K-H, Son BS, Kim H-M, Jeong DH, Jun B-H. 4-Mercaptobenzoic Acid Labeled Gold-Silver-Alloy-Embedded Silica Nanoparticles as an Internal Standard Containing Nanostructures for Sensitive Quantitative Thiram Detection. Int J Mol Sci. 2019;20:4841.
69. Su KH, Wei QH, Zhang X, Mock JJ, Smith DR, Schultz S. Interparticle Coupling Effects on Plasmon Resonances of Nanogold Particles. Nano Lett. 2003;3:1087–90. doi:10.1021/nl034197f.
70. Link S, El-Sayed MA. Spectral Properties and Relaxation Dynamics of Surface Plasmon Electronic Oscillations in Gold and Silver Nanodots and Nanorods. J Phys Chem B. 1999;103:8410–26. doi:10.1021/jp9917648.
71. Josephy PD, Eling T, Mason RP. The horseradish peroxidase-catalyzed oxidation of 3,5,3',5'-tetramethylbenzidine. Free radical and charge-transfer complex intermediates. J Biol Chem. 1982;257:3669–75. doi:https://doi.org/10.1016/S0021-9258(18)34832-4.

72. Li BL, Luo HQ, Lei JL, Li NB. Hemin-functionalized MoS 2 nanosheets: enhanced peroxidase-like catalytic activity with a steady state in aqueous solution. Rsc Advances. 2014;4:24256–62.
73. Ma M, Zhang Y, Gu N. Peroxidase-like catalytic activity of cubic Pt nanocrystals. Colloids Surf A. 2011;373:6–10.
74. Asati A, Kaittanis C, Santra S, Perez JM. pH-Tunable Oxidase-Like Activity of Cerium Oxide Nanoparticles Achieving Sensitive Fluorigenic Detection of Cancer Biomarkers at Neutral pH. Anal Chem. 2011;83:2547–53. doi:10.1021/ac102826k.
75. Ge C, Fang G, Shen X, Chong Y, Wamer WG, Gao X, Chai Z, Chen C, Yin J-J. Facet energy versus enzyme-like activities: the unexpected protection of palladium nanocrystals against oxidative damage. ACS Nano. 2016;10:10436–45.
76. Lin L, Song X, Chen Y, Rong M, Zhao T, Wang Y, Jiang Y, Chen X. Intrinsic peroxidase-like catalytic activity of nitrogen-doped graphene quantum dots and their application in the colorimetric detection of H2O2 and glucose. Analytica chimica acta. 2015;869:89–95.
77. Shah V, Shah S, Shah H, Rispoli FJ, McDonnell KT, Workeneh S, Karakoti A, Kumar A, Seal S. Antibacterial activity of polymer coated cerium oxide nanoparticles. PLoS One. 2012;7:e47827.
78. Frey A, Meckelein B, Externest D, Schmidt MA. A stable and highly sensitive 3,3',5,5'-tetramethylbenzidine-based substrate reagent for enzyme-linked immunosorbent assays. J Immunol Methods. 2000;233:47–56. doi:https://doi.org/10.1016/S0022-1759(99)00166-0.
79. Tian J, Liu S, Luo Y, Sun X. Fe (III)-based coordination polymer nanoparticles: peroxidase-like catalytic activity and their application to hydrogen peroxide and glucose detection. Catal Sci Technol. 2012;2:432–6.
80. Song Y, Qu K, Zhao C, Ren J, Qu X. Graphene Oxide: Intrinsic Peroxidase Catalytic Activity and Its Application to Glucose Detection. Adv Mater. 2010;22:2206–10. doi:https://doi.org/10.1002/adma.200903783.
81. Lipinski B Hydroxyl Radical and Its Scavengers in Health and Disease. *Oxidative Medicine and Cellular Longevity* 2011, *2011*, 809696, doi:10.1155/2011/809696.
82. You L, Mao Y, Ge J. Synthesis of Stable SiO2@Au-Nanoring Colloids as Recyclable Catalysts: Galvanic Replacement Taking Place on the Surface. J Phys Chem C. 2012;116:10753–9. doi:10.1021/jp2119185.
83. Stöber W, Fink A, Bohn E. Controlled growth of monodisperse silica spheres in the micron size range. J Colloid Interface Sci. 1968;26:62–9. doi:https://doi.org/10.1016/0021-9797(68)90272-5.

Figures

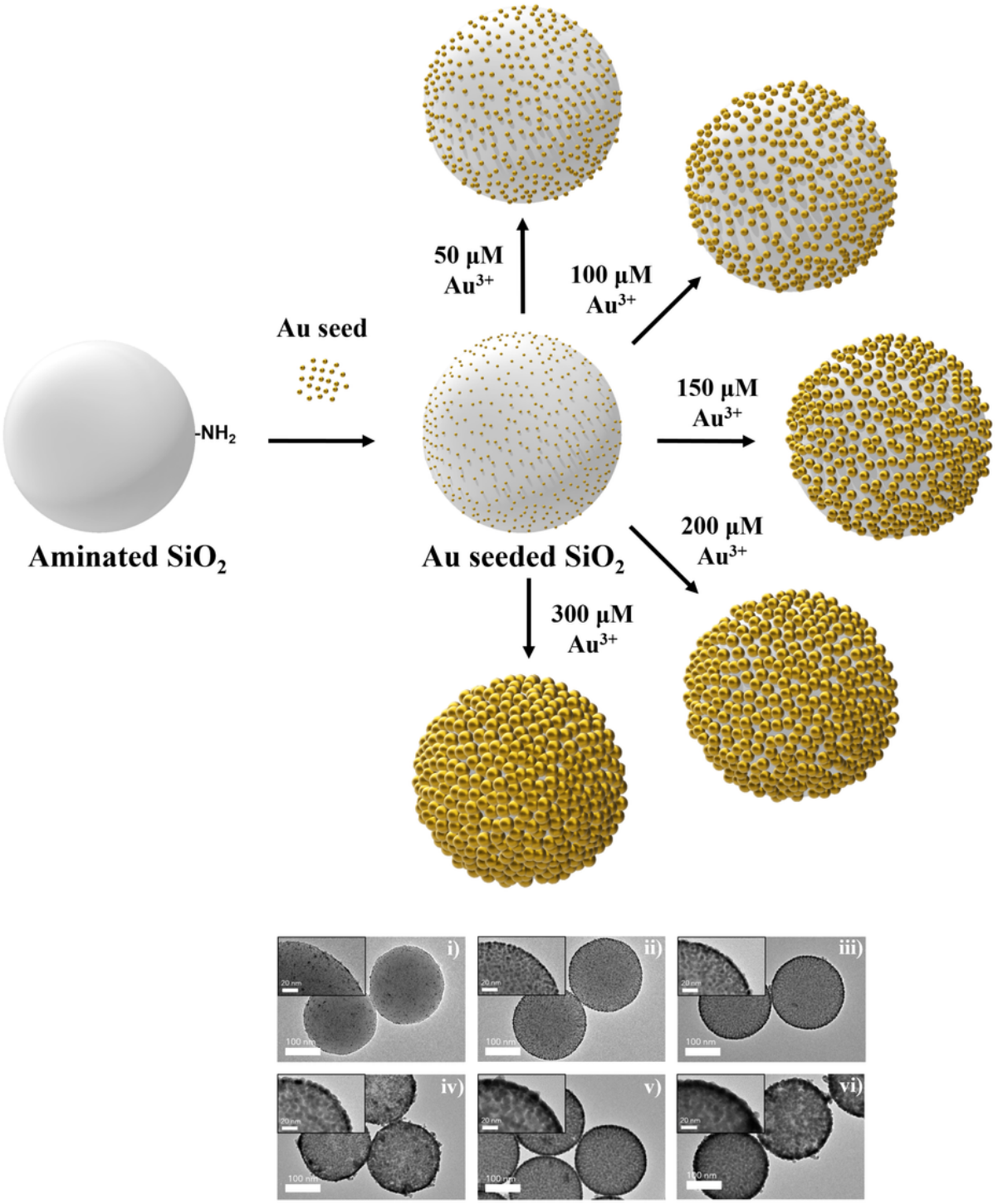

Figure 1

Gold-embedded silica nanospheres (SiO2@Au NPs). a) A schematic representation of synthesis of SiO2@Au NPs. b) The transmission electronic microscopy (TEM) images of SiO2@Au NPs fabricated in various concentrations of Au3+: (i) 0 µM, (ii) 50 µM, (iii) 100 µM, (iv) 150 µM, (v) 200 µM, and (vi) 300 µM.

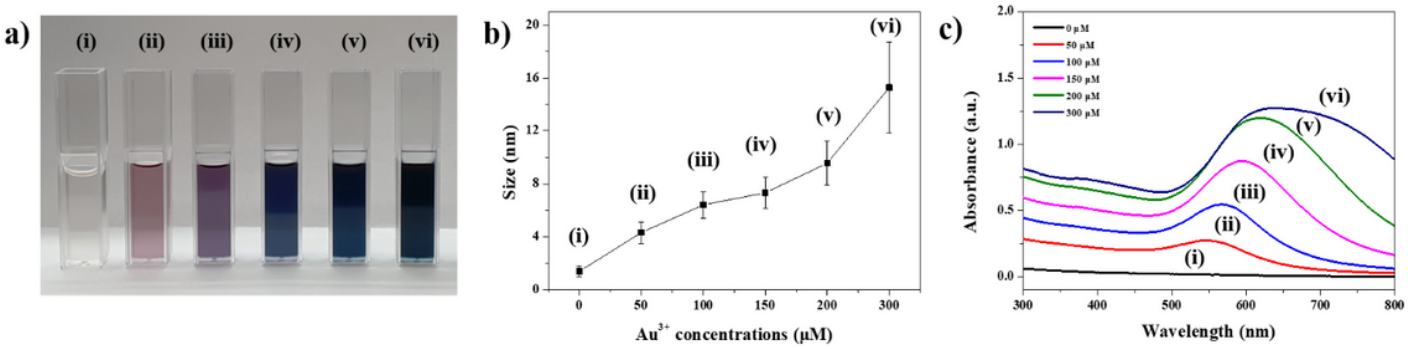

Figure 2

(a) Optical images and (b) Size of Au NPs, and (c) UV-Vis absorption spectra of SiO2@Au NPs fabricated in various concentrations of Au3+ precursor: (i) 0 μM, (ii) 50 μM, (iii) 100 μM, (iv) 150 μM, (v) 200 μM, and (vi) 300 μM.

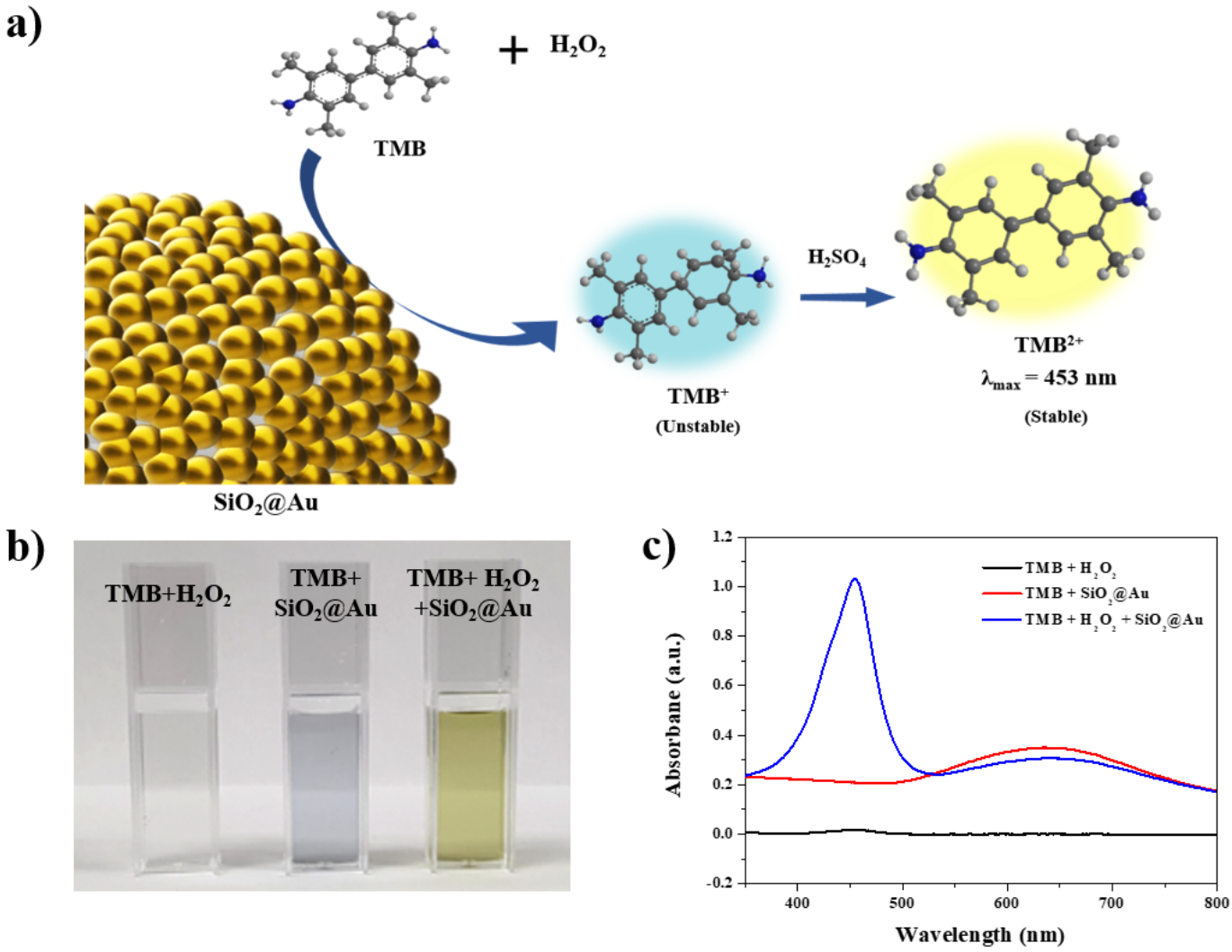

Figure 3

(a) Illustration of the peroxidase-like activity of the SiO2@Au NPs. (b) Optical image and (c) UV-Vis absorption spectra of tetramethylbenzidine (TMB)+H2O2, TMB+SiO2@Au NPs, and TMB+H2O2+SiO2@Au NPs after termination with 1 M H2SO4 in the mixture of 1 mM TMB and 200 mM H2O2. The peak which appeared at 453 nm wavelength originated from the oxidized TMB substrate.

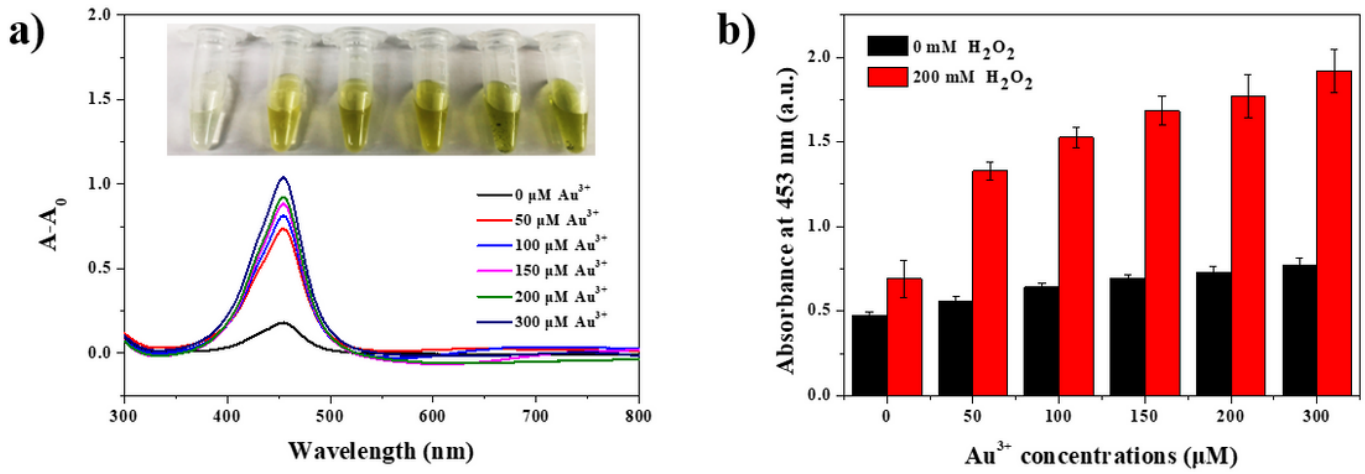

Figure 4

(a) The UV-Vis absorption spectra of subtraction sampled without H2O2 from samples with H2O2 and (b) Absorbance plots of 1 mM TMB and 200 mM H2O2 in the presence of various SiO2@Au NPs fabricated in different Au3+ concentrations in the range of 0 to 300 μM.

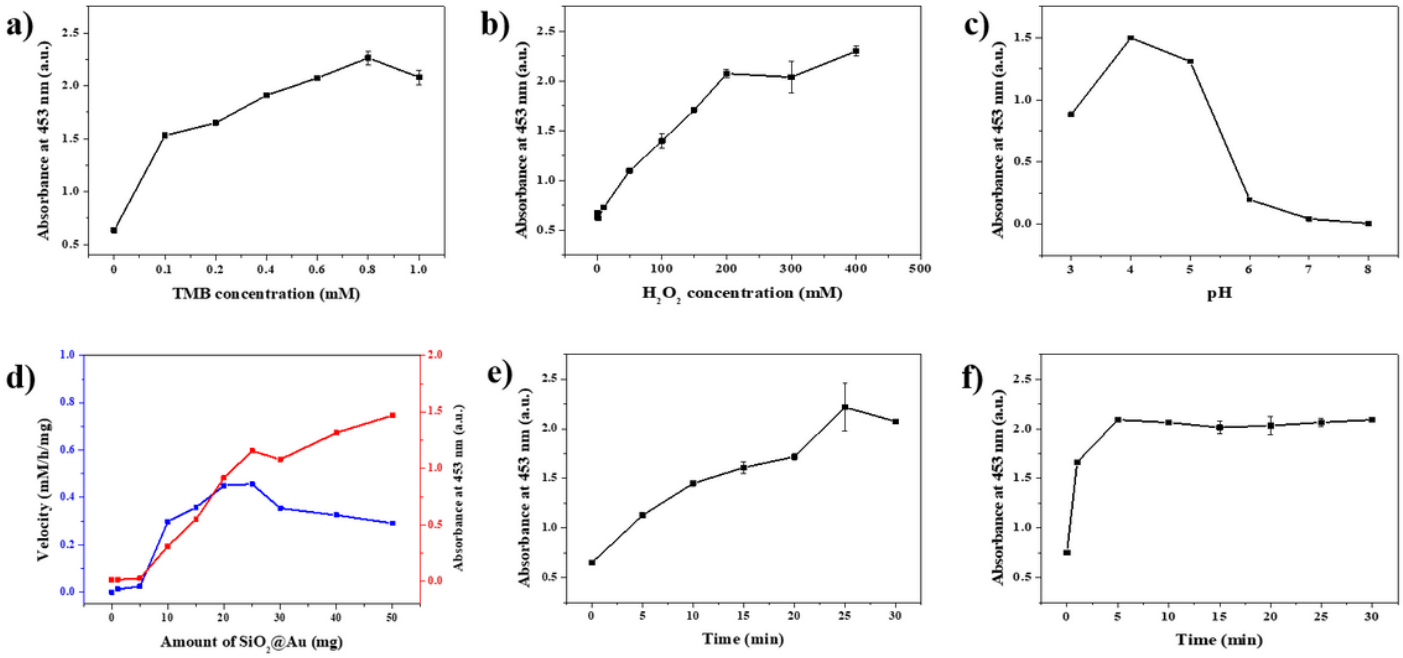

Figure 5

The effects of different reaction conditions on the peroxidase-like activity of SiO2@Au NPs in a mixture of TMB and H2O2. (a) TMB concentration, (b) H2O2 concentration, (c) pH value of the solution, (d) the

velocity and amount of SiO2@Au, (e) reaction time, and (f) termination time.

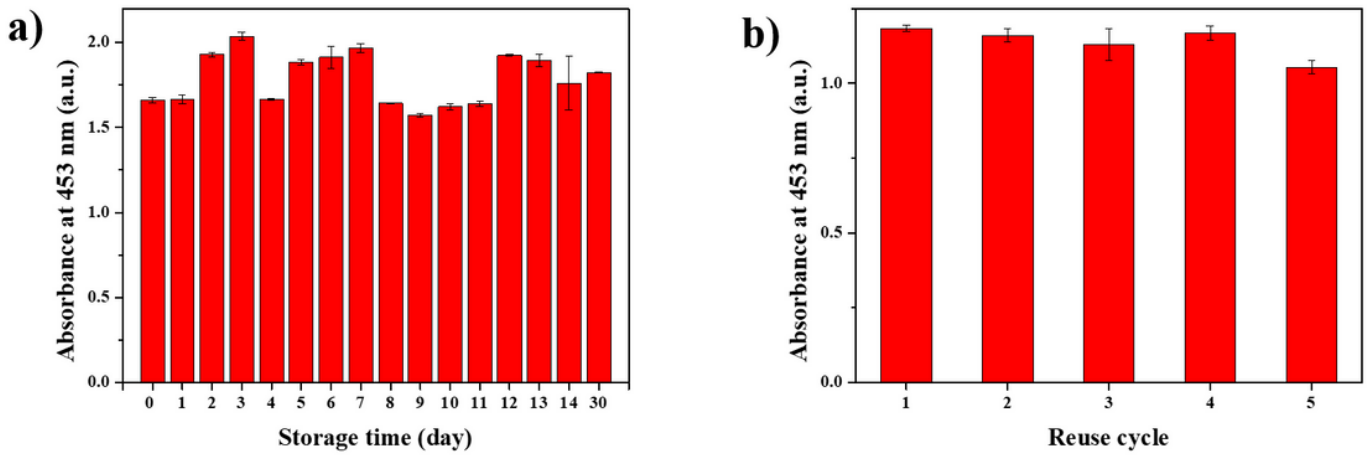

Figure 6

(a) Long-term stability of the peroxidase-like activity and (b) reusability of SiO2@Au NPs in a mixture of 0.6 mM TMB, 200 mM H2O2, and pH 4 buffer. The SiO2@Au NPs were stored in PBST (0.1%) at room temperature.

Supplementary Files

This is a list of supplementary files associated with this preprint. Click to download.

- GraphicAbstract.tif
- Supportinginformation.docx